

Goldman-Hodgkin-Katz equation (GHK-equation)<sup>8</sup>. In the experiment of figure 2A1, the permeability to  $K^+$  ( $P_K$ ) and  $[K^+]_{in}$  were estimated to be  $9.2 \times 10^{-14} \text{ cm}^3/\text{s}$  and  $147 \text{ mM}$  by the least square method. Thus, the  $K^+$  equilibrium potential ( $E_K$ ) was calculated to be  $-97.3 \text{ mV}$ . The mean  $\pm$  SD of  $P_K$  and  $E_K$  were  $9.4 \pm 0.1 \times 10^{-14} \text{ cm}^3/\text{s}$  and  $-96.6 \pm 0.75 \text{ mV}$  ( $n = 4$ ). The slope conductance at  $0 \text{ mV}$  was  $23.2 \pm 5.2 \text{ pS}$  ( $n = 4$ ). In two patches, the reversal of the SL-channel current was obtained when the pipette was filled with  $85 \text{ mM } K^+$  solution (fig. 2A). The reversal potential of them was  $-7.9 \text{ mV}$  and  $-4.2 \text{ mV}$ , and the slope conductance at  $0 \text{ mV}$  was  $34.0 \text{ pS}$  and  $27.3 \text{ pS}$ . The  $I-V$  relationship under such conditions was almost linear (fig. 2A2, triangles) and could be fitted quite reasonably with the GHK-equation using the values of  $P_K$  and  $[K^+]_{in}$  obtained by the fitting of the data in  $3.3 \text{ mM } K^+$ . These results indicate that the SL-channel is a  $K^+$  channel and its outward-rectifying property is due to the constant-field rectification. Although detailed kinetic analyses have not yet been done, the inspection of single channel data revealed that the SL-channel was almost voltage-independent. The activity of the channel was not markedly changed over a wide range of voltages, and the single channel current could be recorded at the hyperpolarized potential as well as the depolarized potential if the driving force for  $K^+$  was appropriate (see the data in  $85 \text{ mM } K^+$  in fig. 2).

The  $I-V$  relationship of the SS-channel was linear (fig. 2B2). When the pipette solution contained  $3.3 \text{ mM } K^+$ , the extrapolated reversal potential was  $-86.4 \pm 12.3 \text{ mV}$  and the single channel conductance was  $8.5 \pm 1.7 \text{ pS}$  ( $n = 13$ ). When the pipette was filled with  $85 \text{ mM } K^+$  solution, the SS-channel current reversed at about  $0 \text{ mV}$  ( $0.0 \pm 3.4 \text{ mV}$ ,  $n = 4$ ) and the single channel conductance was increased to  $17.1 \pm 2.4 \text{ pS}$  ( $n = 4$ ). These results indicate that the SS-channel is also a  $K^+$  channel. In contrast to the SL-channel, the SS-channel was voltage-dependent. Its activity was not seen until the patch potential was depolarized from the resting potential even though the pipette was filled with  $85 \text{ mM } K^+$  solution and the opening probability was clearly increased by the depolarization.

The SL-channel seems to be the homologous channel to the S-channel of *Aplysia* neurones<sup>3-5</sup>. Both the SL-channel of PON and the S-channel of *Aplysia* function over a wide range of voltages near the resting potential and do not inactivate with prolonged depolarization. The  $I-V$  relationship of a single S-channel current also shows the outward rectification and can be fitted by the GHK-equation. Although the

slope conductance at  $0 \text{ mV}$  of the SL-channel (about  $23 \text{ pS}$ ) is less than that of the S-channel (about  $50 \text{ pS}$ ), the published values for the  $P_K$  of the S-channel ( $1.31 \times 10^{-13} \text{ cm}^3/\text{s}$ <sup>3</sup>,  $1.66 \times 10^{-13} \text{ cm}^3/\text{s}$ <sup>4</sup> and  $8.7 \times 10^{-14} \text{ cm}^3/\text{s}$ <sup>5</sup>) are quite similar to the value obtained for the SL-channel of PON ( $9.3 \times 10^{-14} \text{ cm}^3/\text{s}$ ). The difference of the slope conductance may reflect the difference in species.

The SS-channel was the voltage-dependent  $K^+$  channel and its single channel conductance was about  $8.5 \text{ pS}$  in the normal  $K^+$ -gradient. This value and the flickering kinetics of the SS-channel are comparable to those of the delayed rectifier  $K^+$  channel identified in the squid giant axon<sup>9</sup> and the frog skeletal muscle<sup>10</sup>; however, detailed kinetic analyses of the SS-channel still need to be done.

The action of 5-HT on SL- and SS-channels is considered to be mediated by the second messenger system(s), as 5-HT applied by bath perfusion cannot reach the ion channels in the cell-attached patch<sup>6</sup>. In *Aplysia*, several pieces of evidence suggest that the modulation of the S-channel by 5-HT is mediated by a cyclic AMP-dependent protein kinase<sup>11</sup>. The 5-HT-sensitive  $K^+$  current of PON in the whole-cell clamped condition did not reverse in the normal  $K^+$ -gradient and the reversal of this current was not seen until  $[K^+]_{out}$  was raised 5-fold<sup>1</sup> or more. These results reported previously could be explained by the constant-field rectification of the SL-channel current and the voltage dependency of the SS-channel.

- 1 Furukawa, Y., and Kobayashi, M., J. exp. Biol. (1988) in press.
- 2 Klein, M., Camardo, J., and Kandel, E. R., Proc. natl Acad. Sci. USA 79 (1982) 5713.
- 3 Brezina, V., Eckert, R., and Erxleben, C., J. Physiol. (London) 382 (1987) 267.
- 4 Pollock, J. D., and Camardo, J. S., Brain Res. 410 (1987) 367.
- 5 Siegelbaum, S. A., Camardo, J. S., and Kandel, E. R., Nature 299 (1982) 413.
- 6 Hamill, O. P., Marty, A., Neher, E., Sakmann, B., and Sigworth, F. J., Pflügers Arch. 391 (1981) 85.
- 7 Takeuchi, H., Yokoi, I., Mori, A., and Kohsaka, M., Gen. Pharmac. 6 (1975) 77.
- 8 Hodgkin, A. L., and Katz, B., J. Physiol. (London) 108 (1949) 37.
- 9 Conti, F., and Neher, E., Nature 285 (1980) 140.
- 10 Standen, N. B., Stanfield, P. R., and Ward, T. A., J. Physiol. (London) 364 (1985) 339.
- 11 Siegelbaum, S. A., Belardetti, F., Camardo, J. S., and Shuster, M. J., J. exp. Biol. 124 (1986) 287.

0014-4754/88/090738-03\$1.50 + 0.20/0

© Birkhäuser Verlag Basel, 1988

## Ultrastructure and biochemistry of the pineal organ in deep-sea lanternfishes (Myctophidae)

J. A. McNulty, M. A. Neighbors<sup>a</sup> and M. H. Horn<sup>a</sup>

Department of Anatomy, Loyola University Stritch School of Medicine, Maywood (Illinois 60153, USA), and <sup>a</sup> Department of Biological Sciences, California State Fullerton, Fullerton (California 92634, USA)

Received 17 May 1988; accepted 30 May 1988

**Summary.** Pineal structural and biochemical adaptations in lanternfishes included: 1) few photoreceptor outer segment discs; 2) conventional synapses between photoreceptors and pineal neurons; and 3) low levels ( $0-60 \text{ pg/pineal}$ ) of serotonin compared to those ( $> 1.0 \text{ ng/pineal}$ ) in the goldfish pineal organ. These findings suggest reduced photosensory and/or neuroendocrine functions in these deep-sea fishes.

**Key words.** Pineal; serotonin; photoreceptors; synapses; lanternfishes; goldfish.

The pineal gland of poikilothermic vertebrates contains well-differentiated photoreceptors that also have neuroendocrine functions. Indole biosynthetic pathways leading to the con-

version of serotonin (5HT) to melatonin exhibit circadian rhythms with peak enzymatic activities occurring during the dark phase<sup>1</sup>. This functional relationship to photoperiodic

Levels of 5HT and 5HIAA (ng/pineal) in the goldfish and myctophids

	5HT	5HIAA
<i>Carassius auratus</i>	1.14 <sup>a</sup> ± 0.15	0.82 <sup>a</sup> ± 0.11
<i>Triphoturus mexicanus</i>	0.06	0.01
<i>Stenobranchius leucopsaurus</i>	0.06	0.04
<i>Lampanyctus ritteri</i>	0.04	0.01
<i>Tarletonbeania crenularis</i>	0.02	0.01
<i>Symbolophorus californiensis</i>	nd <sup>b</sup>	nd <sup>b</sup>

<sup>a</sup> means (± SEM) from 5 glands; <sup>b</sup> not detectable.

input prompted the present investigation of pineal structure and biochemistry in deep-sea fishes that inhabit an environment where light is absent, or nearly so.

**Methods.** Species of lanternfishes (family Myctophidae) listed in the table were collected at a depth of approximately 450 m during daylight and 0–450 m at night from a deep basin off southern California. For electron microscopic and biochemical analyses of their pineal organs, the roof of the skull with pineal organs attached was removed with a razor blade and either immediately frozen on dry ice or immersion fixed in 4% glutaraldehyde buffered with 0.1 M monosodium phosphate (pH 7.4). For comparative purposes, pineal glands of goldfish (*Carassius auratus*) were also collected and examined.

Tissues collected for electron microscopy were dissected from the calvaria, post-fixed in phosphate buffered 1% OsO<sub>4</sub>, dehydrated in a graded series of acetone and embedded in epoxy resin. Thin sections were examined with an Hitachi H-600 electron microscope.

Pineal levels of serotonin (5HT) and 5-hydroxyindole acetic acid (5HIAA) were measured by high performance liquid chromatography (HPLC) as previously described<sup>2,3</sup>. Briefly, glands were homogenized in 0.1 N perchloric acid, centrifuged, and the supernatant injected into the chromatograph consisting of an Altex 110 A metering pump, a Rheodyne inject port and a Bioanalytical LC-4B electrochemical controller with the potential of the working electrode set at +0.8 V relative to the Ag/AgCl reference electrode. The mobile phase was 0.1 M sodium phosphate (pH 4.5) mixed with 15% (v/v) methanol delivered at 1.0 ml/min. Preliminary studies revealed that 5HT and 5HIAA levels were not detectable in individual myctophid glands. Therefore, for any one species of lanternfish, from 8 to 38 glands

were pooled for a single injection. All indoles of interest were detectable in single goldfish pineals.

**Results and discussion.** Pineal glands of all species comprised photoreceptor, supportive, and ganglion cells, which is consistent with prior reports<sup>4–6</sup>. Compared to the goldfish, myctophids had fewer photoreceptor outer segment discs (figs 1 and 2), and ganglion cells (fig. 3) were less frequently observed. Furthermore, synaptic ribbons, which were present exclusively in the goldfish neuropil (fig. 4), were never observed in myctophids. Instead, 'typical' synapses occurred at contact sites between myctophid photoreceptors and ganglion cell dendrites (Inset, fig. 3). Pre-synaptic terminals were identified as photoreceptor processes based on the appearance of the mitochondria. The synapses had pre- and postsynaptic membrane specializations with clear vesicles (40–50 nm in diameter) in the presynaptic photoreceptor terminal. To our knowledge, this is the first report of conventional photoreceptor-neuronal synaptic contacts in the teleost pineal organ, and is a notable exception to the usual occurrence of synaptic ribbons in photoreceptors. Conventional synapses have been described in the pineal organ of other teleosts<sup>7</sup>, but these were axo-axonic (neuronal-photoreceptor) contacts. The functional significance of conventional vs ribbon synapses in pineal photoreceptors is not clear<sup>8</sup>.

Serotonin and 5HIAA were detectable in pooled glands of most myctophid species (table), but pineal levels of these indoles were between 2% and 5% of levels found in the goldfish. Size of the gland cannot account for these species differences in indole content since the volume of the pineal end-vesicle in the goldfish was similar to the pineal volume in *T. mexicanus*<sup>6,9</sup>. These findings may suggest a relationship between low levels of pineal indoles and decreased environmental lighting. However, the eel (*Anguilla*), a species that inhabits rivers and streams during part of its life cycle, has pineal 5HT levels (0–10 pg/gland)<sup>10</sup> similar to deep-sea, dark-adapted lanternfishes. Moreover, light adaptation appears to decrease pineal 5HT content in the eel and the goldfish<sup>3,10</sup>.

Serotonin, besides being a precursor to melatonin, has also been considered as a putative neurotransmitter. Spontaneous electrophysiological activity of more than half the pineal neurons in a frog are inhibited by iontophoretically applied 5HT<sup>11</sup>, which is taken up and immunocytochemically localized within photoreceptor cells<sup>3,12</sup>. The relation-

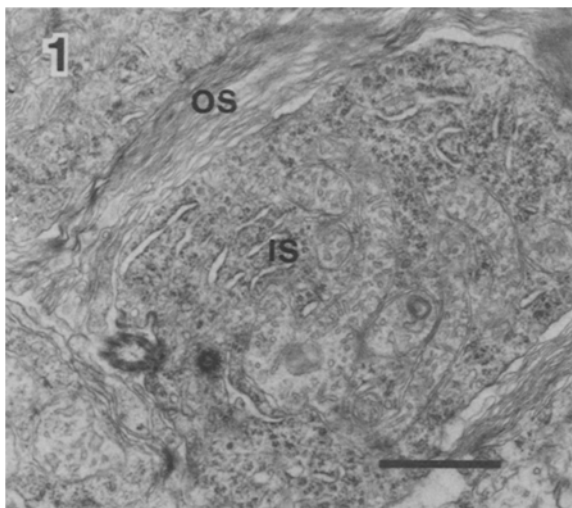


Figure 1. Outer segment saccules (OS) and inner segment (IS) of photoreceptor in pineal organ of *T. crenularis*. Bar indicates 1 µm.

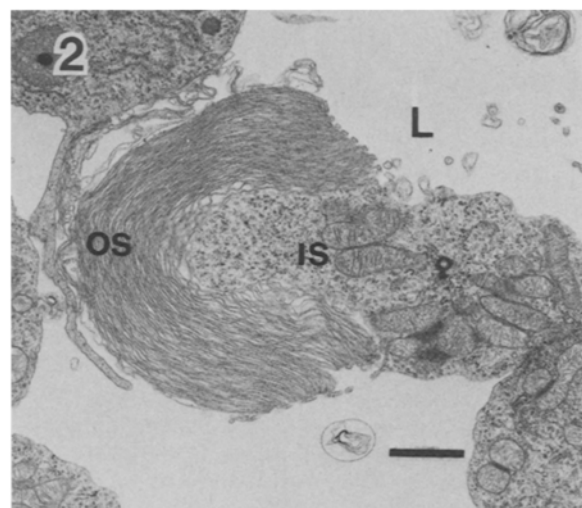


Figure 2. Goldfish photoreceptor protruding into the central lumen (L) of the pineal organ. Bar indicates 1 µm.

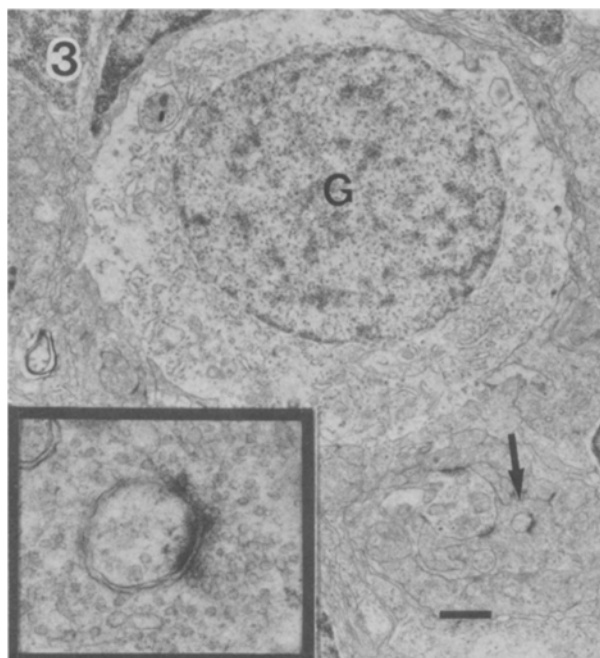


Figure 3. A ganglion cell (G) in the pineal of *S. californiensis* is seen bordering a small neuropil (arrow). Bar indicates 1  $\mu$ m. Inset: Higher magnification of synapse depicted by arrow.

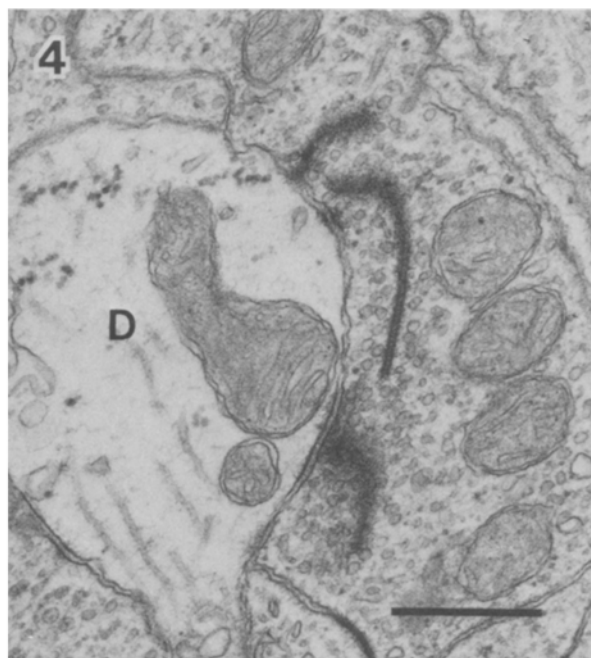


Figure 4. Several goldfish photoreceptor synaptic ribbons contacting a ganglion cell dendrite (D). Bar indicates 0.5  $\mu$ m.

ship between pineal levels of 5HT and the predominance of synaptic ribbons in the neuropil is unclear with respect to differences in the innervation of the pineal organ in the goldfish and myctophids.

In view of the wide variation in pineal morphology<sup>13</sup>, it is noteworthy that the present biochemical findings reflect to some extent the structural diversity reported in the pineal complex of myctophids<sup>5</sup>. Lanternfishes that contained greater amounts of 5HT (*T. mexicanus*, *S. leucopsaurus*, *L. ritteri*) have pineal complexes characterized by a prominent central lumen in the end-vesicle and a dorsal sac. By comparison, *T. crenularis* and *S. californiensis*, which tended to have lower levels of 5HT, are species that have compact pineal end-vesicles and lack a dorsal sac.

To summarize, it appears from the present study that structural and biochemical adaptations of the pineal organ to low light levels probably involve both photosensory and neuroendocrine functions in these deep-sea fishes.

- 1 Falcon, J., Guerlotte, J. F., Voison, P., and Collin, J. P., *Neuroendocrinology* 45 (1987) 479.
- 2 McNulty, J. A., *Cell Tissue Res.* 238 (1984) 565.
- 3 McNulty, J. A., *Gen. comp. Endocr.* 61 (1986) 179.
- 4 McNulty, J. A., and Nafpaktitis, B. G., *J. Morph.* 150 (1976) 579.
- 5 McNulty, J. A., and Nafpaktitis, B. G., *Am. J. Anat.* 150 (1977) 509.
- 6 McNulty, J. A., *Can. J. Zool.* 59 (1981) 1312.
- 7 Omura, Y., and Ali, M. A., *Cell Tissue Res.* 208 (1980) 111.
- 8 Korf, H.-W., *Cell Tissue Res.* 174 (1976) 475.
- 9 McNulty, J. A., *Cell Tissue Res.* 172 (1976) 205.
- 10 van Veen, Th., Laxmyr, L., and Borg, B., *Gen. comp. Endocr.* 46 (1982) 322.
- 11 Meissl, H., and George, R., *Vision Res.* 24 (1984) 1727.
- 12 Falcon, J., Geffard, M., Juillard, M. T., Steinbusch, H. W. M., Sequela, P., and Collin, J. P., *J. Histochem. Cytochem.* 32 (1984) 486.
- 13 Vollrath, L., *The Pineal Organ, Handbuch der Mikroskopischen Anatomie des Menschen*, VI/7. Springer-Verlag, Berlin 1981.

0014-4754/88/090740-03\$1.50 + 0.20/0  
© Birkhäuser Verlag Basel, 1988

## Effect of diabetes on the enzymes of the cholinergic system of the rat brain<sup>1</sup>

Z. Z. Wahba and K. F. A. Soliman<sup>2</sup>

College of Pharmacy and Pharmaceutical Sciences, Florida A & M University, Tallahassee (Florida 32307, USA)  
Received 3 March 1988; accepted 14 June 1988

**Summary.** Choline acetyltransferase (ChAT) and acetylcholinesterase (AChE) activities were determined in several brain regions of normal and streptozotocin-induced diabetic rats. The diabetic rats exhibited significant increase in ChAT activity ( $p < 0.05$ ) in all brain regions studied except for the cortex and the midbrain. Meanwhile, the diabetes condition was associated with significant increase ( $p < 0.05$ ) in AChE activity of the bulbous olfactorius, medulla oblongata and cerebellum. These data suggest that uncontrolled diabetes is associated with significant alterations in the brain cholinergic systems.

**Key words.** Choline acetyltransferase; acetylcholinesterase; brain; diabetes.